13th International Conference on
Structural Health Monitoring of Intelligent Infrastructure
DOI: 10.3217/978-3-99161-057-1-048

Perspectives on vision-based bridge vibrational monitoring by drones

Tommaso Panigati[1, 0009-0001-4077-8058], Pier Francesco Giordano[1, 0000-0003-0396-0253], Daniel Tonelli[2, 0000-0002-9089-4583], Maria Pina Limongelli[1,3, 0000-0002-9353-5439], Daniele Zonta[2, 0000-0002-7591-9519]
[1] Politecnico di Milano, Department of Architecture, Built environment and Construction engineering, Piazza Leonardo da Vinci 32, 20133 Milan, Italy
[2]University of Trento, Department of Civil, Environmental and Mechanical Engineering, Via Mesiano 77, 38123 Trento, Italy
[3]Lund University, Faculty of Engineering, John Ericssons väg 1, Lund, Sweden
email: tommaso.panigati@polimi.it, pierfrancesco.giordano@polimi.it, daniel.tonelli@unitn.it, mariagiuseppina.limongelli@polimi.it, daniele.zonta@unitn.it

ABSTRACT: Vision-based vibrational monitoring aims to extract the modal parameters of civil structures—such as natural frequencies—from recorded video data for Structural Health Monitoring (SHM) purposes. The use of drones for vision-based vibrational monitoring is particularly promising, as drones can access vantage points for video recording that may otherwise be difficult to reach. However, certain drawbacks exist, including potential limitations in resolution, stability, and environmental sensitivity. This paper explores the capabilities, opportunities, and limitations of using drones for vision-based vibrational monitoring. To evaluate technological limits, a target with controlled displacement is used to test various combinations of target distances, displacement amplitudes, and displacement frequencies. Additionally, factors such as environmental conditions and drone hardware are considered. The study defines the practical limits of this approach, aiming to determine the minimum displacement of a vibrating bridge that can be detected by drones. Case studies from the literature are used as benchmarks to identify the dynamic properties of different types of bridges.

KEY WORDS: drones, structural health monitoring, computer vision

1. INTRODUCTION

The deterioration of transportation infrastructure and the limited availability of resources have made Structural Health Monitoring (SHM) essential for supporting bridge management. Within the framework of SHM, vibrational monitoring relies on the global dynamic response of a structure —typically extracting modal parameters such as natural frequencies and mode shapes— to identify damage [1]. Traditionally, vibrational monitoring is performed using fixed systems installed on structures. However, the high cost of components and maintenance makes this approach viable only for a limited number of bridges [2] . Therefore, there is a growing demand for affordable, reliable, portable, and reusable SHM instrumentation to reduce monitoring costs. Among emerging sensing technologies, commercial devices such as smartphones, cameras, drones, and robotic sensors present promising applications [3]. For instance, smartphones can gather vibrational measurements with embedded accelerometers [4]. Moreover, advancements in computer vision techniques enable the extraction of displacement and vibrational data from videos recorded by commercial smartphone and drone cameras [5]. While smartphones and fixed cameras need the physical presence of an operator to record videos close to the target point, drones can be controlled remotely and can reach vantage viewpoints without compromising operator safety [6]. Moreover, in addition to vibrational measurements, drones can gather 2D images of multiple bridge components during the same inspecting session. When combined with advanced computer vision and machine learning techniques, these images can enable a fast and efficient system for surface damage and crack detection [7], [8] However, being flying objects, drones experience in-flight vibrations and unwanted movements (referred as egomotion) that may interfere with their ability to record small structural vibrations of the bridge. As highlighted in [9], there is still the need to assess the field of applicability of commercial drone technology for bridge dynamic identification. The goal of this study is to evaluate the capabilities and limitations of drone-based vision systems for vibrational monitoring. The final scope is to define the practical limits of their application in identifying the dynamic behavior of bridges. Two stages are involved. Firstly, a literature survey identifies the typical range of frequencies and displacements for bridges with different materials, structural typology and span. Secondly, experimental tests are performed to assess the limits of applicability of vision-based approach using drones. The results of the tests are compared with the displacement and frequency range exhibited by real-scale bridges.

This paper is structured as follows. Section 2 describes the typical range of vibrational displacements and frequencies for different types of bridges. These ranges are then compared in section 3 with drone vision-based system capabilities determined with laboratory tests. Results are critically discussed in section 4 while section 5 presents conclusions. The overall flowchart is shown in Figure 1.

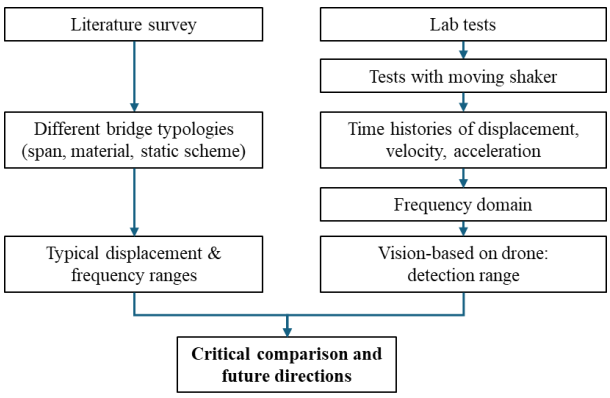

Figure 1: flowchart of the paper.

DOI: 10.3217/978-3-99161-057-1-048

2. LITERATURE SURVEY

This section reviews existing literature to evaluate the typical behavior of bridges in terms of deflections and natural frequencies. This preliminary analysis, combined with the results presented in Section 3, will support the assessment of the feasibility of a vision-based approach using drones. Table 1 presents displacement and frequencies data for various types of bridges, including pedestrian bridges, masonry bridges, concrete bridges, and cable-stayed bridges. The row of the table are organized in ascending order based on the length of the main span. Deflections are divided into static and dynamic: static deflections are caused by the quasi-static presence of the load (for instance a truck when the truck itself is on the bridge), while dynamic deflections are the residual free-vibration amplitudes experienced around the static deflection baseline and once the load is released. This distinction is important because static deflections are typically an order of magnitude larger than dynamic deflections, making them easier to measure. However, static deflections are not suitable for the dynamic characterization of the bridge (i.e., extraction of natural frequencies). For this purpose, dynamic deflections during the transient period after unloading are typically used. In Table 1, static deflections are presented with a positive sign, meaning they are pointing downwards, while dynamic deflections are reported with the ± sign, referring to their oscillation around the static deflection. It is possible to observe

Table 1. Vibrational displacements and frequencies of different types of bridges, ordered by main span length.

Reference	Bridge Type and main span [m]	Load type	Static deflection [mm]	Dynamic deflection [mm]	First natural frequency [Hz] and mode type	Second natural frequency [Hz] and mode type	Measurement type
[10]	Masonry Arch Bridge, 7.7	Train (weight of each boogie 34 ton)	< 1	n.a.	n.a.	n.a.	Fibre Bragg Grating cables and Digital Image Correlation
[11]	Concrete bridge, first span 13.7	2-axle truck a 3-axle bus	0.25 (truck) and 0.45 (bus)	< ±0.05	n.a.	n.a.	Fiber Optics and camera
[12]	Steel-concrete bridge, 19	32-ton truck	3	< ±0.04	n.a.	n.a.	LVDT and accelerometers
[13]	Pedestrian bridge, 23	Pedestrians (single jump)	n.a.	± 2	3.86	5.87	Vision-Based on drone
[14]	Steel road bridge, 25	Heavy trucks	6	± 1.5	3	n.a.	Vision-Based fixed
[15]	Pedestrian bridge, 27	Single person jumping	n.a.	± 2	2.98 (bending)	3.70 (torsional)	Vision-Based
[16]	Concrete, 32	Heavy trucks	< 5	±1	3.48	n.a.	Vision-Based
[17]	Continuous steel-concrete bridge, 40+40	40-ton truck	< 41	±1	2.7 (not specified)	4.7 (not specified)	Vision-Based, on drone, corrected with on-camera accelerometers
[18]	Continuous steel bridge, 4x45	30-ton and 40-ton truck	<5	< ±0.5	Between 2 and 3	n.a.	Vision-Based
[19]	PC railway bridge, 50	High-speed train	1.5	< ±0.2	3.19 (symmetric bending)	3.87 (torsional)	Laser velocity displacement transducer (LVDT)
[6]	Suspended pedestrian bridge, 67	Pedestrians (jumping)	n.a.	±15mm	n.a.	0.5	Vision-Based on drone
[20]	Concrete Bridge, 110	8-ton truck	5.65	n.a.	n.a.	n.a.	Vision-Based on drone
[21]	Single tower suspension bridge, 248	Heavy truck	40	n.a.	n.a.	n.a.	Vision-Based
[17]	Cable-stayed railway bridge, 432	High-speed train and freight train	30 (high-speed) and 75 (freight)	<±3	0.336 (vertical bending)	0.764 (vertical bending)	Vision-Based, corrected with on-camera accelerometers, distance 150 m
[22]	Suspended bridge, 1410 (main span)	2x heavy trucks	200	n.a.	n.a.	n.a.	Vision-Based fixed camera

DOI: 10.3217/978-3-99161-057-1-048

the significant variation of the displacement range (from <1 mm to ≈200 mm) for different combinations of span and stiffness. All the deflections are caused by defined forcing loading conditions (for instance a truck or a train). Conversely, vibrations caused by environmental solicitations are generally too small to be detected by a vision-based system [23]. This poses a challenge for dynamic extraction, as the time frame valid for the extraction of modal parameters is just limited within a few seconds after the excitation. Moreover, the loading itself may present some peculiar periodicity that is not related to the bridge, therefore affecting the result with spurious peaks in the spectral content. This is the case of trains passing over a bridge, where the periodicity is given by boogies passing over the sampling point [19], or of people walking over a pedestrian bridge, where walking has specific frequency.

Table 1 also presents the first two identified frequencies, when available. The peaks of the bridge frequency spectrum should be compared with the dominant peaks of the drone egomotion spectrum. If the bridge frequency peak overlaps with the drone egomotion peak, it becomes more difficult to accurately capture the dynamic behavior of the bridge using drones.

From Table 1, it emerges that, when a conventional load such as a heavy truck passes, static deflections are between 1/20000 and 1/5000 of the bridge span, while dynamic deflections are between 1/50000 and 1/10000 of the bridge span. These estimates provide a useful reference for the expected vibration amplitudes of a bridge and help define the range of applicability of the vision-based approach using drones presented in Section 3.

3. LABORATORY TESTS

The laboratory tests were conducted using a commercial DJI MINI 2 drone, which was directed at a moving target oscillating vertically. Two experimental setups were tested. In the first setup, the moving target was simulated on a screen, representing a concrete-like surface with a sinusoidal displacement time history in the vertical direction, controlled by user-defined displacement amplitude and frequencies. In the second setup, the target was a physical point subjected to vertical sinusoidal displacement driven by a pre-programmed shaker, see Figure 2. The tests aim to determine under which conditions the input (known) oscillation frequencies can be identified from the resulting time-domain and frequency-domain plots. For the video-target case, displacements ranged from ±0.25 mm to ±10 mm, with frequencies between 0.5 Hz and 15 Hz. For the physical-target case, displacements ranged from ±0.5 mm to ±2.5 mm, with frequencies between 1 Hz and 5 Hz. In both cases, the drone, with its camera recording the target, was flown at varying distances between 1.5 m and 10 m. Different video lengths were tested, ranging from 10 to 60 s. Videos were recorded in 4K resolution (3840 × 2160) at 30 frames per second (fps). Tests were conducted both indoors and outdoors, yielding similar results. Under outdoor conditions, the increased drone oscillations caused by gentle wind gusts were compensated for by more accurate positioning provided by the Global Navigation Satellite System (GNSS). In both cases, also a fixed target was tracked for the sake of measuring the drone egomotion.

From the recorded video, a script using Kanade-Lucas-Tomasi tracking [24], [25], was employed to extract the time history of vertical and horizontal displacements. From these displacement data, velocities and acceleration were also computed. Finally, the Fast Fourier Transform (FFT) algorithm was applied to the displacement, velocity, and acceleration data to analyze their frequency content.

Figure 2 presents the results of a test conducted in the second setup. In the test, the drone was flown at a distance of 10 m, recording the vertical oscillation of the target, which had an amplitude of ± 2.5 mm (total range 5 mm) and a frequency of 3 Hz. In Figure 3, time histories of displacements, velocities and accelerations of a fixed reference target (orange) and the oscillating target (blue) are shown, in both horizontal (X) and vertical (Y) direction. The displacement of the fixed target is exclusively due to drone egomotion. The low-frequency

(a) (b)

Figure 2. Experimental setup: (a) Drone and targets; (b) Detail of targets.

DOI: 10.3217/978-3-99161-057-1-048

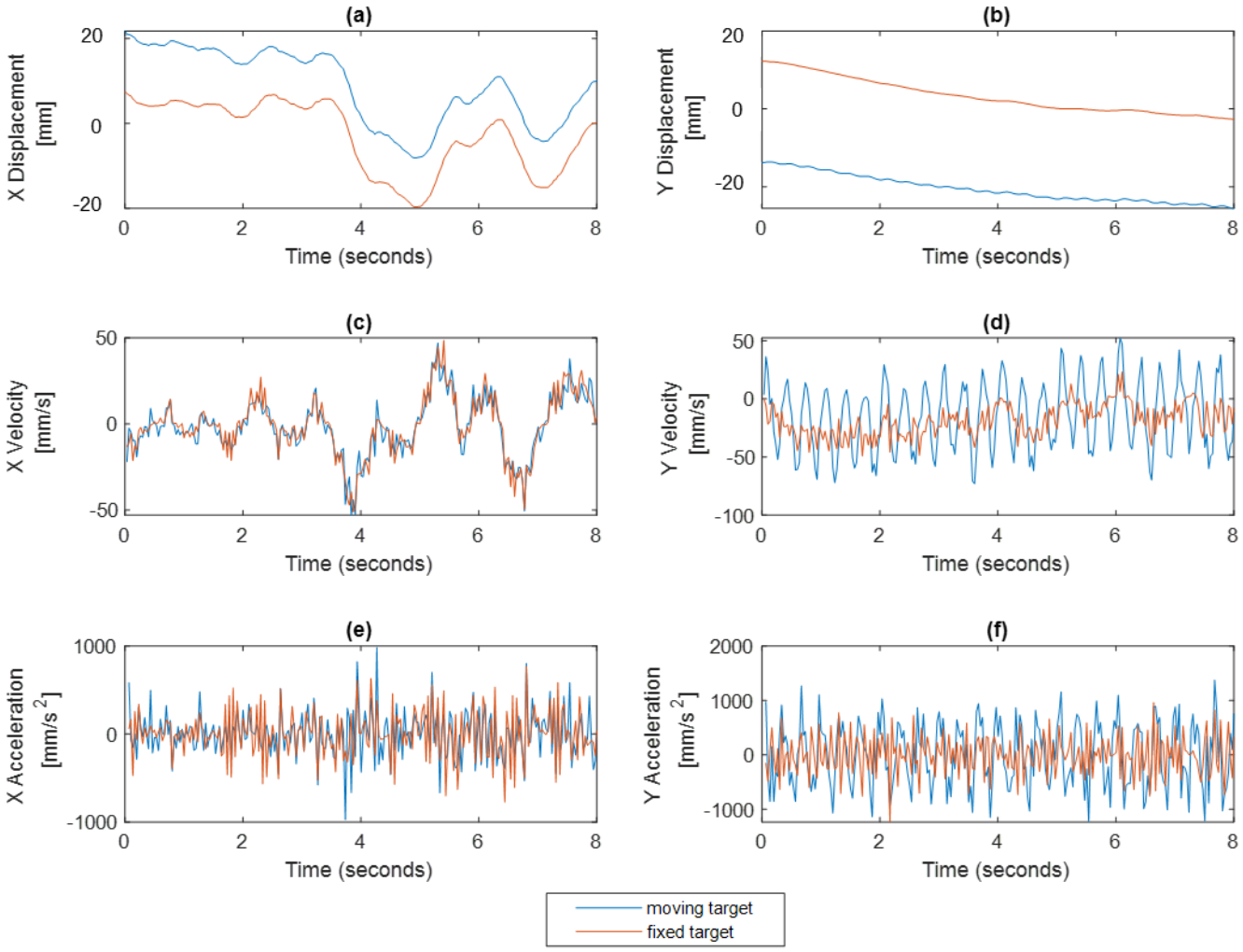

Figure 3. Time histories for a point with 5 mm / 3 Hz oscillation; drone camera at 10 m distance. Time histories of: displacement, (a) x direction and (b) y direction; velocity, (c) x direction and (d) y direction; acceleration, (e) x direction and (f) y direction.

oscillations, especially in the X direction, are due to drone egomotion. Conversely, high frequency vibrations of the moving target are due to the shaker user-defined vibrations. Figure 3 shows spectra of displacement (a), velocity (b) and acceleration (c) in horizontal and vertical direction, for the time histories shown in Figure 2. In Figure 3, a prominent peak in the frequency spectrum of the vertical acceleration and velocity corresponds to the shaker's oscillation frequency.

Results from all the tests provide valuable insights. In particular, some quantities have proven more effective for analyzing the results. Spectra of acceleration and velocity are less sensitive to low-frequency disturbances, resulting in sharp and easily detectable peaks. Conversely, spectra of displacement tend to present less distinct peaks near the frequency of interest. As the frequency of the input excitation increases, the spectrum of acceleration becomes clearer, while the spectrum of velocity becomes less distinct. As a general rule, if the spectrum of acceleration does not allow for capturing the peak, the spectra of velocity and displacement are unlikely to succeed either. For this reason, the spectrum of acceleration is used as the primary means for identifying the frequency of interest.

The results are summarized in presence of moderate noise, yet low enough to avoid missing real and distinguishable peaks. Results confirm that for the range of frequency above 3 Hz the performance of vision-based tracking is optimal, and sub-millimetric displacements can be captured. On the other hand, at lower frequencies, the drone non-compensated egomotion (which typically falls within the 0–2 Hz range) negatively

DOI: 10.3217/978-3-99161-057-1-048

affects the results. In this low-frequency range, only displacements with larger amplitudes are detectable if egomotion compensation are applied. Drones with better optics might have a wider range of detectable displacements, while heavier drone might suffer less from egomotion disturbance.

Table 2, where the comparison is shown for a distance of 1.5 m, that is a compromise between optical precision and safety distance to avoid collision, using data from both setups. For simplicity, the results have been categorized into two groups: Yes (Y) when the peak in the acceleration spectrum was clearly visible, and No (N) when the identification was uncertain. There are several criteria for peak detection [26]. In this study, the criterion used to distinguish between Yes and No involved calculating the ratio between the peak value and the average signal in the spectrum. If the ratio exceeded 5, the result was marked as Yes; otherwise, it was marked as No. The threshold of 5 was selected because it is high enough to allow clear identification of the peak even in the presence of moderate noise, yet low enough to avoid missing real and distinguishable peaks. Results confirm that for the range of frequency above 3 Hz the performance of vision-based tracking is optimal, and sub-millimetric displacements can be captured. On the other hand, at lower frequencies, the drone non-compensated egomotion (which typically falls within the 0–2 Hz range) negatively affects the results. In this low-frequency range, only displacements with larger amplitudes are detectable if egomotion compensation are applied. Drones with better optics might have a wider range of detectable displacements, while heavier drone might suffer less from egomotion disturbance.

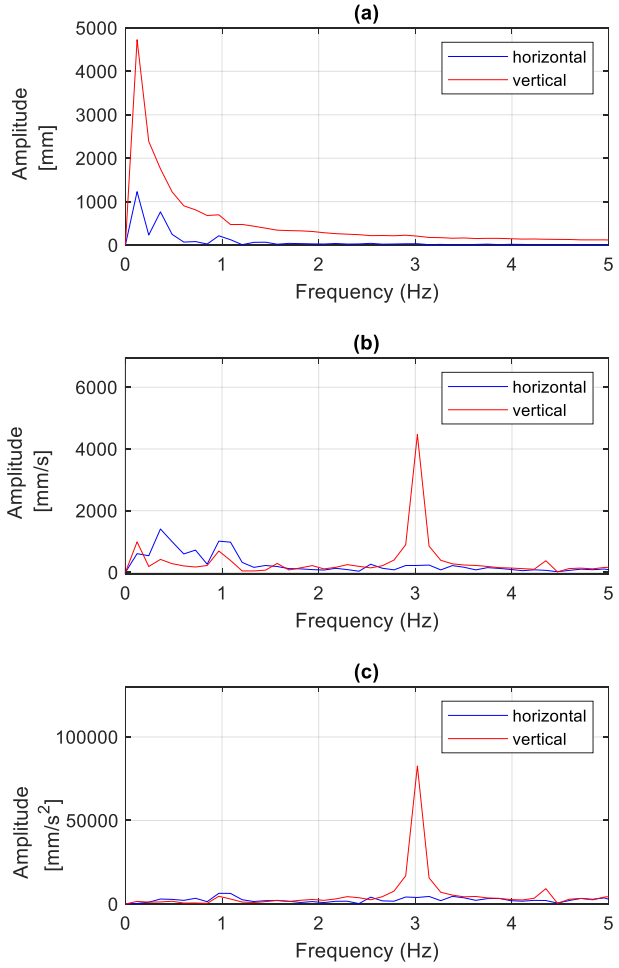

Figure 4. Spectra of (a) displacement, (b) velocity, (c) acceleration, for horizontal (X) and vertical (Y) displacement, calculated using FFT algorithm, for a point with 5 mm / 3 Hz oscillation; drone camera at 10 m distance.

Table 2. Range of detectability of frequencies.

		Frequency [Hz]						
		0.5	1	2	3	7	10	13
Displ. [mm]	±0.25	N	N	N	Y	Y	Y	Y
	±0.50	N	N	N	Y	Y	Y	Y
	±0.75	N	N	N	Y	Y	Y	Y
	±1.00	N	N	Y	Y	Y	Y	Y
	±5	N	N	Y	Y	Y	Y	Y
	±10	N	Y	Y	Y	Y	Y	Y

4. CRITICAL DISCUSSION

The results obtained in section 3 can be critically compared with the data presented in section 2. When a heavy load passes over a bridge, the resulting static displacement is typically a few millimeters; once the load is released, the amplitude of free vibrations usually falls below 2-5 mm. In a controlled laboratory test, a low-cost drone demonstrated the ability to detect the dynamic behavior of vertically oscillating targets even for oscillations of less than 1 mm, provided that the free vibration frequency is above 2 Hz — allowing for the decoupling of drone egomotion from target vibrations. Based on these findings, drones might be capable of identifying the first frequency of selected bridges, provided that (i) the bridge is loaded by a heavy vehicle, (ii) the bridge is sufficiently flexible, and (iii) its first natural frequency does not coincide with the dominant frequencies of the drone's egomotion. Given those constraints, bridges that might be suitable for the capability of the existing drone technology are:

- Pedestrian bridges spanning more than 20 m, as those presented in [13], [15];
- Slender mid-span concrete and steel bridges, spanning more than 40 m, as those presented in [16], [17].

Conversely, short-span bridges and arch bridges of all materials are typically too stiff to exhibit significant displacement. Moreover, long-span suspended and cable-stayed bridges typically have low frequency modes that overlap with drone egomotion peaks, hindering vision-based dynamic identification with drones. It must be remarked that results from Table 2 are based on a controlled environment with sinusoidal oscillations; in contrast, the free vibrations of real bridges are less regular and, therefore, more challenging to be captured.

It must also be noted that the experiment was performed using an entry level commercial drone, weighing less than 250 g and costing less than 500€. Using a superior category drone could improve the results for three key reasons: (i) higher quality camera, (ii) reduced oscillations due to increased weight, and (iii) more stable hovering with enhanced gimbal stabilization. A list of suitable drones with their specifications is provided in Table 3. It must be remarked that drone weighting less than 250

DOI: 10.3217/978-3-99161-057-1-048

grams can be flown with less restrictions in European Union, while heavier drones typically require pilot training.

Table 3. Commercial drone specifications.

Model	Year	Weight (g)	Camera	Obstacle Avoidance	Cost (€)
DJI Mini 2	2020	249	12 MP, 4 K/30 fps	Downward	~450
DJI Mini 4 Pro	2024	249	48 MP, 4 K/60 fps; HDR	Omni-directional	~800
Autel Evo Nano +	2023	249	50 MP, 4 K/30 fps	Forward/ Backward	~800
Potensic Dreamer Pro	2022	745	12 MP, 4 K/30 fps	None	~500
DJI Air 3	2023	720	24 MP wide + 5 × tele	Omni-directional	~1,100
DJI Mavic 3 Pro	2022	895	4/3″ 20 MP + tele + wide	Omni-directional	~2,100

Results could be improved by applying inertial-based egomotion compensation using data from accelerometers [6] or vision-based egomotion compensation using external reference points, such as background features [27]. However, most commercial drones, including the DJI MINI 2, do not allow access to accelerometric data, making inertial-based egomotion compensation unfeasible.

5. CONCLUSIONS

This study presented a comparison between bridge dynamic behavior and capabilities of drone vision-based dynamic monitoring. The literature review assessed the typical dynamic displacement ranges of bridge with varying length, material and static scheme. Laboratory tests validated the usage of vision-based dynamic monitoring on drones for vibrations happening with frequencies above 2 Hz and displacement ranges above 1 mm. These values match with properties of pedestrian bridges and of slender mid-span concrete and steel bridges. Further on-field tests should be conducted to verify the applicability to real cases. Improving egomotion compensation is expected to enhance the accuracy of dynamic identification using drones. The need to perform dynamic monitoring, with the constraint of the presence of a passing vehicle, introduces new challenges, such as the need to perform vibrational monitoring using very short and transient time histories, which falls outside the traditional framework of operational modal analysis.

ACKNOWLEDGMENTS

This work was supported by PRIN: PROGETTI DI RICERCA DI RILEVANTE INTERESSE NAZIONALE – Bando 2022, under grant number Prot. 2022P44KA8, provided by the Italian Ministry of Education, Universities and Research. This work was financed by European Union - Next Generation EU, Mission 4 Component 1 CUP D53D23003870006.

REFERENCES

[1] M. Modesti, C. Gentilini, A. Palermo, E. Reynders, and G. Lombaert, “A two-step procedure for damage detection in beam structures with incomplete mode shapes,” *J Civ Struct Health Monit*, 2024, doi: 10.1007/s13349-024-00839-0.

[2] P. F. Giordano, S. Quqa, and M. P. Limongelli, “The value of monitoring a structural health monitoring system,” *Structural Safety*, vol. 100, 2023, doi: 10.1016/j.strusafe.2022.102280.

[3] S. Sony, S. Laventure, and A. Sadhu, “A literature review of next-generation smart sensing technology in structural health monitoring,” *Struct Control Health Monit*, vol. 26, no. 3, 2019, doi: 10.1002/stc.2321.

[4] E. Figueiredo, I. Moldovan, P. Alves, H. Rebelo, and L. Souza, “Smartphone Application for Structural Health Monitoring of Bridges,” *Sensors*, vol. 22, no. 21, 2022, doi: 10.3390/s22218483.

[5] C. Ferraris, G. Amprimo, and G. Pettiti, “Computer Vision and Image Processing in Structural Health Monitoring: Overview of Recent Applications,” *Signals*, vol. 4, no. 3, 2023, doi: 10.3390/signals4030029.

[6] V. Hoskere, J.-W. Park, H. Yoon, and B. F. Spencer, “Vision-Based Modal Survey of Civil Infrastructure Using Unmanned Aerial Vehicles,” *Journal of Structural Engineering (United States)*, vol. 145, no. 7, 2019, doi: 10.1061/(ASCE)ST.1943-541X.0002321.

[7] S. Feroz and S. A. Dabous, “Uav-based remote sensing applications for bridge condition assessment,” *Remote Sens (Basel)*, vol. 13, no. 9, 2021, doi: 10.3390/rs13091809.

[8] S. Jiang, Y. Cheng, and J. Zhang, “Vision-guided unmanned aerial system for rapid multiple-type damage detection and localization,” *Struct Health Monit*, vol. 22, no. 1, pp. 319–337, 2023, doi: 10.1177/14759217221084878.

[9] T. Panigati *et al.*, “Drone-based bridge inspections: Current practices and future directions,” *Autom Constr*, vol. 173, p. 106101, May 2025, doi: 10.1016/J.AUTCON.2025.106101.

[10] S. Acikgoz, M. J. . DeJong, C. Kechavarzi, and K. Soga, “Dynamic response of a damaged masonry rail viaduct: Measurement and interpretation,” *Eng Struct*, vol. 168, 2018, doi: 10.1016/j.engstruct.2018.04.054.

[11] D. Lydon, M. Lydon, S. Taylor, J. M. Del Rincon, D. Hester, and J. Brownjohn, “Development and field testing of a vision-based displacement system using a low cost wireless action camera,” *Mech Syst Signal Process*, vol. 121, 2019, doi: 10.1016/j.ymssp.2018.11.015.

[12] D. Hester, J. Brownjohn, M. Bocian, and Y. Xu, “Low cost bridge load test: Calculating bridge displacement from acceleration for load assessment calculations,” *Eng Struct*, vol. 143, 2017, doi: 10.1016/j.engstruct.2017.04.021.

[13] Y. Bai, H. Sezen, A. Yilmaz, and R. Qin, “Bridge vibration measurements using different camera placements and techniques of computer vision and deep learning,” *Advances in Bridge Engineering*, vol. 4, no. 1, 2023, doi: 10.1186/s43251-023-00105-1.

DOI: 10.3217/978-3-99161-057-1-048

[14] Z. Aliansyah, K. Shimasaki, T. Senoo, I. Ishii, and S. Umemoto, "Single-camera-based bridge structural displacement measurement with traffic counting," *Sensors*, vol. 21, no. 13, 2021, doi: 10.3390/s21134517.
[15] T. Panigati, A. Abbozzo, M. A. Pace, E. Temur, F. Cigan, and R. Kromanis, "Dynamic Identification of Bridges Using Multiple Synchronized Cameras and Computer Vision," *Infrastructures (Basel)*, vol. 10, no. 2, 2025, doi: 10.3390/infrastructures10020037.
[16] F. Micozzi, M. Morici, A. Zona, and A. Dall'Asta, "Vision-Based Structural Monitoring: Application to a Medium-Span Post-Tensioned Concrete Bridge under Vehicular Traffic," *Infrastructures (Basel)*, vol. 8, no. 10, 2023, doi: 10.3390/infrastructures8100152.
[17] T. Wu *et al.*, "Accurate structural displacement monitoring by data fusion of a consumer-grade camera and accelerometers," *Eng Struct*, vol. 262, 2022, doi: 10.1016/j.engstruct.2022.114303.
[18] J. J. Lee and M. Shinozuka, "A vision-based system for remote sensing of bridge displacement," *NDT and E International*, vol. 39, no. 5, 2006, doi: 10.1016/j.ndteint.2005.12.003.
[19] H. Xia, G. De Roeck, N. Zhang, and J. Maeck, "Experimental analysis of a high-speed railway bridge under Thalys trains," *J Sound Vib*, vol. 268, no. 1, 2003, doi: 10.1016/S0022-460X(03)00202-5.
[20] S. Ri, J. Ye, N. Toyama, and N. Ogura, "Drone-based displacement measurement of infrastructures utilizing phase information," *Nat Commun*, vol. 15, no. 1, 2024, doi: 10.1038/s41467-023-44649-2.
[21] Y. Han, G. Wu, and D. Feng, "Vision-based displacement measurement using an unmanned aerial vehicle," *Struct Control Health Monit*, 2022, doi: 10.1002/stc.3025.
[22] J. M. W. Brownjohn, Y. Xu, and D. Hester, "Vision-based bridge deformation monitoring," *Front Built Environ*, vol. 3, 2017, doi: 10.3389/fbuil.2017.00023.
[23] K. Luo, X. Kong, J. Zhang, J. Hu, J. Li, and H. Tang, "Computer Vision-Based Bridge Inspection and Monitoring: A Review," *Sensors*, vol. 23, no. 18, 2023, doi: 10.3390/s23187863.
[24] B. D. Lucas and T. Kanade, "ITERATIVE IMAGE REGISTRATION TECHNIQUE WITH AN APPLICATION TO STEREO VISION.," in *7th joint international conference on Artifical Intelligence*, Vancouver, 1981.
[25] C. Tomasi, "Detection and Tracking of Point Features," *School of Computer Science, Carnegie Mellon Univ.*, vol. 91, no. April, 1991.
[26] G. K. Palshikar, "Simple Algorithms for Peak Detection in Time-Series Simple Algorithms for Peak Detection in Time-Series," *Design*, no. July, 2002.
[27] H. Yoon, J. Shin, and B. F. Spencer, "Structural Displacement Measurement Using an Unmanned Aerial System," *Computer-Aided Civil and Infrastructure Engineering*, vol. 33, no. 3, 2018, doi: 10.1111/mice.12338.